High-Power 980-nm DFB RW Lasers With a Narrow Vertical Far Field

H. Wenzel, J. Fricke, A. Klehr, A. Knauer, and G. Erbert, *Member, IEEE*

***Abstract*—We compare 980-nm distributed-feedback ridge-waveguide lasers having cavity lengths of 1.5 and 3 mm. The maximum single-mode output powers are 500 and 700 mW, respectively. The full-width at half-maximum of the vertical far-field profile is only 22° due to a superlarge optical cavity.**

***Index Terms*—Distributed feedback (DFB) lasers, ridge waveguides (RWs), semiconductor lasers.**

I. Introduction

HIGH-POWER diode lasers emitting in the spectral region around 980 nm are of particular interest for the pumping of erbium- and ytterbium-doped fibers and waveguides. Today's devices provide 500 mW coupled in a single-mode fiber. In order to increase the pump power to 1 W and above, several pump lasers can be combined using polarization and wavelength combiners. Since the absorption window of erbium is less than 10 nm around 980 nm, the pumping wavelengths must be carefully chosen and stabilized. The use of distributed feedback (DFB) lasers instead of Fabry–Pérot lasers coupled to fiber Bragg gratings (FBGs) is one possible solution. DFB lasers offer also the possibility to integrate several frequency stabilized pump sources and erbium-doped waveguides on a single chip without the need of aligning and fusing many FBGs which makes sophisticated packaging unnecessary and the devices more compact.

DFB lasers emitting at 976 nm could also replace certain argon ion lasers ($\lambda = 488$ nm) by frequency doubling using periodically poled $LiNbO_3$ or KTP crystals. All of these applications require a high spatial-mode purity in the lateral far field in addition to the high spectral purity of the lasing emission. Furthermore, in order to reduce the facet load and to facilitate a low-cost coupling to fibers and waveguides, the vertical far-field divergence should be lowered as much as possible.

A conventional fundamental-mode DFB laser has a narrow stripe and a Bragg grating that is oriented perpendicular to the propagation direction and to the facet normal. In contrast, the angled grating (α) DFB laser is a broad-area device in which the grating is oriented parallel to the propagation direction and is tilted by an angle of about 10° with respect to the facets normal. The angled grating provides both spectral and spatial mode control. Although α-DFB lasers are capable to emit a power of more than 1 W, they suffer from a kinky light–current characteristic and a low efficiency [1]. A fiber-coupled power of 400 mW at a current of 2.5 A was achieved [2].

Conventional fundamental-mode DFB lasers emitting around 980 nm were already presented in [3], [4], and [5] with output powers of 58, 75, and 200 mW, respectively. We reported high-power DFB ridge-waveguide (RW) lasers in [6] and [7], where a continuous-wave (CW) power of 200 mW at 780 nm and of 300 mW at 860 nm was achieved. In [8], we presented a 980-nm emitting DFB RW laser with a maximum single-mode output power of almost 400 mW. In this letter, we report on DFB RW lasers emitting between 975 and 980 nm, with more than 700-mW single-mode output power.

II. Structure and Fabrication

For lasers emitting in the desired wavelength region, AlGaAs or InGaAsP heterostructures can be employed. Owing to the high affinity of aluminum to oxygen, an Al-containing surface exposed to air can hardly be overgrown in a conventional metal–organic vapor phase epitaxy reactor which complicates the fabrication of a Bragg grating integrated into the layer structure. On the other hand, the growth of AlGaAs is well established. For these reasons, AlGaAs is employed for the confinement and cladding layers whereas the Bragg grating is formed in an Al-free layer sequence.

The growth of the layer structure and the fabrication of the Bragg grating takes place as follows. The first growth step consists of n-GaAs buffer, n-$Al_{0.70}Ga_{0.30}As$, n-$Al_{0.45}Ga_{0.55}As$ waveguide, the active layer, the first part of the p-$Al_{0.45}Ga_{0.55}As$ confinement and the InGaP–GaAsP–InGaP layer sequence. The first-order Bragg grating with a period around 150 nm is formed in this layer sequence by holographic photolithography and wet-chemical etching. A frequency quadrupled Nd : YAG laser with an emission wavelength of $\lambda = 266$ nm is used in the holographic setup. In the second step the remainder of the p-$Al_{0.45}Ga_{0.55}As$ confinement layer, the p-$Al_{0.70}Ga_{0.30}As$ cladding layer and the p-GaAs contact layer are grown. The active layer consists of a compressively strained InGaAs single quantum well sandwiched between GaAsP spacers. A coupling coefficient of 2 cm^{-1} was determined by fitting amplified spontaneous emission spectra measured below threshold to a parameterized theoretical model.

Lateral optical confinement is provided by a 2.2-μm-wide dry-etched RW with an effective-index step of $\Delta n_{\text{eff}} = 0.002$. After processing, the wafers are cleaved into bars with lasers having cavity lengths of $L = 1.5$ mm and $L = 3$ mm. The front and rear facets are anti- and high-reflection coated, respectively, and the bars are cleaved into single laser chips. At the

Manuscript received September 27, 2005; revised January 2, 2006. This work was supported by Zukunftsfond Berlin.

The authors are with the Ferdinand-Braun-Institut für Höchstfrequenztechnik, 12489 Berlin, Germany (e-mail: wenzel@fbh-berlin.de).

Digital Object Identifier 10.1109/LPT.2006.871127

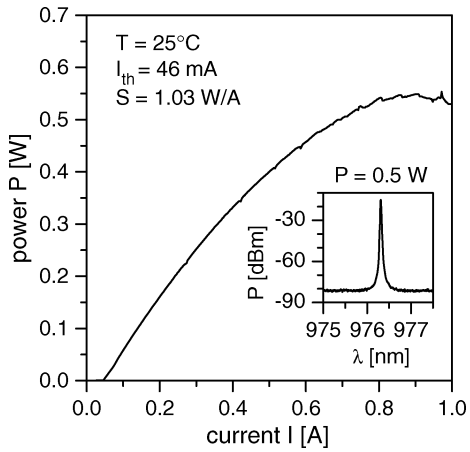

Fig. 1. CW light–current characteristics of a 1.5-mm-long DFB RW laser. Inset: optical spectrum at an output power 500 mW.

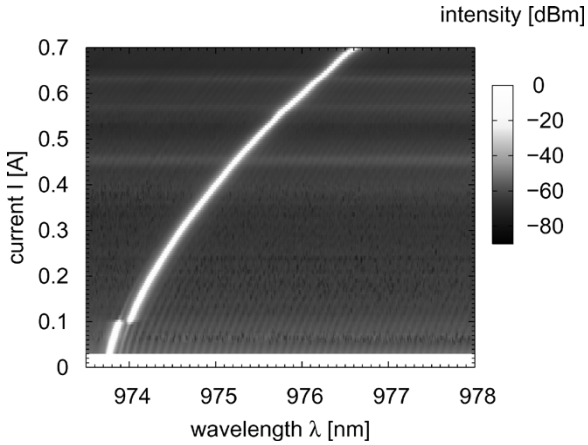

Fig. 2. Color-scale plot of the optical spectrum of the device of Fig. 1 versus current.

front facets, the reflection coefficients are typically below 10^{-3}. For the CW measurements, the chips covered with electroplated gold are soldered p-down on CuW submounts by exploiting the AuSn ζ phase [9] and finally mounted on C-mounts. Preliminary lifetime tests at 500-mW output power and 25 °C heat sink temperature indicate a good reliability of lasers mounted in such a way.

III. Device Characteristics

We present results first for the 1.5-mm-long device in Figs. 1–3 and then for the 3-mm-long device in Figs. 4 and 5.

As can be seen in Fig. 1, the maximum output power of the 1.5-mm-long device is 540 mW and it is limited by thermal rollover. The light–current characteristic is kink-free up to 500-mW output power. The optical spectrum depicted in the inset of Fig. 1 reveals single-longitudinal-mode operation at 500 mW with a sidemode suppression ratio of 60 dB.

A mapping of the optical spectrum is depicted in Fig. 2. It shows that single-mode operation is maintained over a large current range from slightly above threshold (46 mA) up to 700 mA, except around a current of 100 mA where a mode hop from the short- to the long-wavelength side of the stopband can be observed. The nonlinear increase of the lasing wavelength seen in

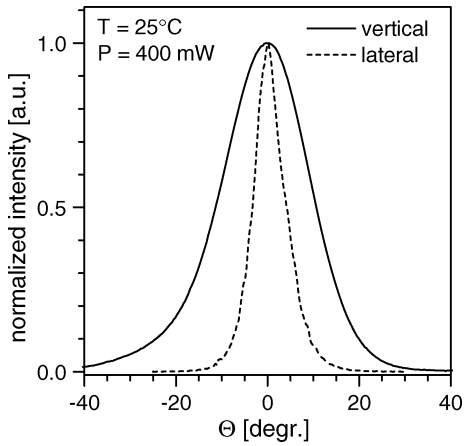

Fig. 3. Vertical (solid) and lateral (dashed) far-field profiles of the device of Fig. 1 at an output power of 400 mW.

Fig. 2 is caused by the temperature-induced change of the refractive indexes, mainly due to Joule heating. From the wavelength variation of about $\Delta\lambda = 2.7$ nm between 50 and 700 mA, a temperature rise of $\Delta T = 40$ K can be deduced on the basis of a temperature coefficient of $\Delta\lambda/\Delta T = 0.0675$ nm/K determined near threshold. Together with the dissipated power (not shown here), a thermal resistance of 18.9 W/K can be estimated.

A closer inspection of the light–current characteristics in Fig. 1 unveils several small dips below 500 mW which can be explained as follows. The tuning of the wavelength with current leads to a scanning of absorption lines of atoms or molecules present in the laboratory's air. If the laser wavelength coincides with one of these lines, owing to the power loss, a dip in the light–current characteristics is created. In the wavelength range between 970 and 980 nm, there are several absorption lines of water vapor. A more detailed discussion can be found in [6].

Owing to the superlarge optical cavity (SLOC) with a total width of the $Al_{0.45}Ga_{0.55}As$ confinement layers of 3.6 μm, the vertical far field is very narrow, as can been seen in Fig. 3. Full-width at half-maximum (FWHM) angle is only 22°. It is slightly larger than that of comparable Fabry–Pérot lasers with the same SLOC structure, but no grating layers (FWHM 18°). The lateral far-field profile also shown in Fig. 3 reveals fundamental lateral mode operation with an FWHM of 7.5°.

The threshold current of the 3-mm-long DFB RW laser is only slightly increased from 46 to 50 mA compared to the 1.5-mm-long device. The slope efficiency determined slightly above threshold decreased from 1 to 0.8 W/A due to the longer cavity. Nevertheless, Fig. 4 shows that at a current of 1500 mA, an output power of 970 mW is reached. The reason is that the longer cavity causes a decrease of the thermal resistance resulting in a reduced thermal rollover in the investigated power range.

The light–current characteristics is kink-free up to 700-mW output power. The optical spectrum depicted in the inset of Fig. 4 reveals single-longitudinal mode operation at 700 mW with a sidemode suppression ratio of 60 dB.

The mapping of the optical spectrum of the 3-mm-long device depicted in Fig. 5 exhibits regions of stable single-mode operation bounded by instability regions. The spectral broadening of the lasing line in these regions is associated with regular and

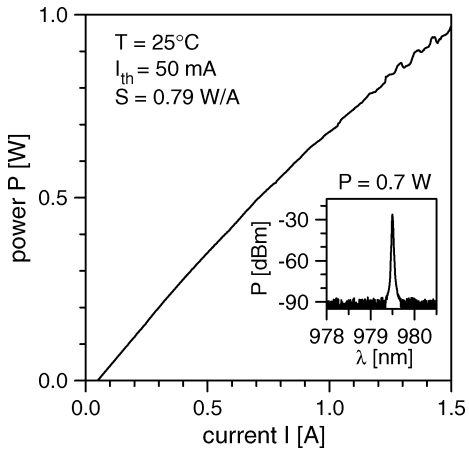

Fig. 4. CW light–current characteristics of a 3-mm-long DFB RW laser. Inset: optical spectrum at an output power 700 mW.

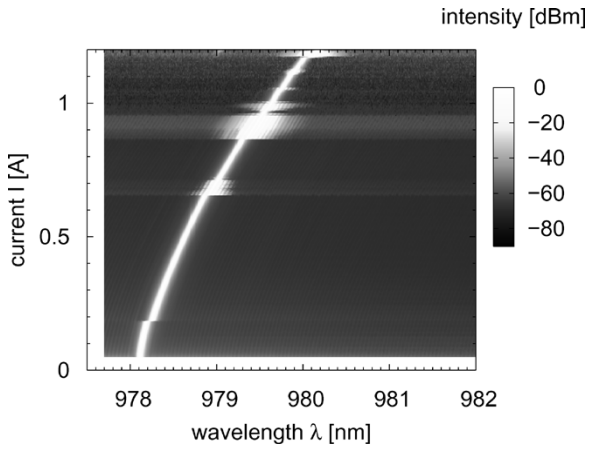

Fig. 5. Color-scale plot of the spectrum of the device of Fig. 4 versus current.

irregular self-pulsing of the laser. The repetition frequency determined with an electrical spectrum analyzer varies between 1.1 and 1.4 GHz. The origin of this self-pulsating behavior is not understood yet.

There is again a mode hop around 180 mA. The temperature rise of 30 K deduced from the wavelength variation of about 2.0 nm between 100 and 1200 mA is much smaller than for the 1.5-mm-long device due to the reduced thermal resistance of 10.5 K/W.

IV. Summary

We have demonstrated stable single-longitudinal mode operation of DFB RW lasers at output powers of 500 and 700 mW for cavity lengths of 1.5 and 3 mm, respectively. Due to the SLOC, the FWHM of the vertical far-field profile is only 22°. The 1.5-mm-long device exhibits a mode-hop free tuning range of 2.5 nm over a current range of 600 mA (corresponding power range 440 mW). For the 3-mm-long laser, regions of stable-single-mode operation are bounded by instability regions.

References

[1] K. Paschke, A. Bogatov, F. Bugge, A. E. Drakin, J. Fricke, R. Güther, A. A. Stratonikov, H. Wenzel, G. Erbert, and G. Tränkle, "Properties of ion.implanted high-power angled-grating distributed feedback lasers," *IEEE J. Sel. Topics Quantum Electron.*, vol. 9, no. 5, pp. 1172–1178, Sep./Oct. 2003.

[2] S. D. De Mars, T. Oeskevitch, A. Schoenfelder, and R. Lang, "400-mW single-mode fiber-coupled DFB laser at 980 nm," in *Tech. Dig. CLEO'97*, 1997, Paper CMA2, p. 2.

[3] Y. K. Sin and H. Horikawa, "High power 0.98 μm InGaAs-GaAs-InGaP distributed feedback buried heterostructure strained quantum well lasers," *Electron. Lett.*, vol. 29, pp. 920–922, 1993.

[4] D. T. Nichols, J. Lopata, W. S. Hobson, P. F. Sciortino Jr., and N. K. Dutta, "DFB and DBR lasers emitting at 980 nm," *Electron. Lett.*, vol. 29, pp. 2035–2037, 1993.

[5] R. M. Lammert, J. E. Ungar, S. W. Oh, H. Qi, and J. S. Chen, "High-power InGaAs-GaAs-AlGaAs distributed feedback lasers with nonabsorbing mirrors," *Electron. Lett.*, vol. 34, pp. 886–887, 1998.

[6] H. Wenzel, A. Klehr, M. Braun, F. Bugge, G. Erbert, J. Fricke, A. Knauer, M. Weyers, and G. Tränkle, "High-power 783 nm distributed-feedback laser," *Electron. Lett.*, vol. 40, pp. 123–124, 2004.

[7] H. Wenzel, M. Braun, J. Fricke, A. Klehr, A. Knauer, P. Ressel, G. Erbert, and G. Tränkle, "High-power ridge-waveguide distributed-feedback lasers emitting at 860 nm," *Electron. Lett.*, vol. 38, pp. 1676–1677, 2002.

[8] H. Wenzel, A. Klehr, M. Braun, F. Bugge, G. Erbert, J. Fricke, A. Knauer, P. Ressel, B. Sumpf, M. Weyers, and G. Tränkle, "Design and realization of high-power DFB lasers," *Proc. SPIE*, vol. 5594, pp. 110–123, 2004.

[9] W. Pittroff, G. Erbert, G. Beister, F. Bugge, A. Klein, A. Knauer, J. Maege, P. Ressel, J. Sebastian, R. Staske, and G. Tränkle, "Mounting of high power laser diodes on boron nitride heat sinks using an optimized Au/Sn metallurgy," *IEEE Trans. Adv. Packag.*, vol. 24, no. 4, pp. 434–441, Nov. 2001.